Influence of ZnO nanocrystals surface modification on structure and photovoltaic properties of MEH-PPV/*nc*-ZnO nanocomposite films

N.V.Babayevskaya, Yu.N.Savin, O.O.Matvienko, V.V.Varchenko[*], A.P.Kryshtal[*], M.F.Prodanov[*], Yu.A.Gurkalenko[**], V.V.Vaschenko[*], V.P.Seminozhenko

Institute for Single Crystals, SSI "Institute for Single Crystals", National Academy of Sciences of Ukraine, 60 Lenin Ave., 61001 Kharkiv, Ukraine
[*]Division of Chemistry of Functional Materials, SSI "Institute for Single Crystals", National Academy of Sciences of Ukraine, 60 Lenin Ave., 61001 Kharkiv, Ukraine
[**]Institute for Scintillation Materials, SSI "Institute for Single Crystals", National Academy of Sciences of Ukraine, 60 Lenin Ave., 61001 Kharkiv, Ukraine

The influence of interface modifires based on perylen imide dyes and naphthyl phosphonic acid on MEH-PPV/*nc*-ZnO nanocomposite films morphology was stydied. The better phase compatibility between MEH-PPV and *nc*-ZnO was obtained if (PI1) and (PI2) were used as the IMs. Use of the IMs led to decrease the fluorescence lifetime quenching (τ_1) and to increase the quenching efficiencies (η_q). It was demonstrated that all IMs increase J_{SC} and V_{OC} .

Исследовано влияние интерфейсных модификаторов на основе перилена и нафтил фосфоновой кислоты на морфологию пленок MEH-PPV/*nc*-ZnO. Наилучшая фазовая совместимость наблюдалась для MEH-PPV и *nc*-ZnO при использовании модификаторов (PI1) и (PI2). Использование модификаторов приводит к снижению тушения времени жизни флуоресценции (τ_1) и увеличению эффективности переноса заряда (η_q). Показано, что использование всех модификаторов привело к увеличению J_{SC} и V_{OC}.

***Вплив модифікації поверхні нанокристалів ZnO на структуру та фотовольтаїчні властивості нанокомпозитних плівок MEH-PPV/nc-ZnO.** Н.В.Бабаєвська, Ю.М.Саввін, О.О.Матвієнко, В.В.Варченко, О.П.Кришталь, М.Ф.Проданов, Ю.О.Гуркаленко, В.В.Ващенко, В.П.Семіноженко.*

Досліджено вплив інтерфейсних модифікаторів на основі перилену та нафтилфосфонової кислоти на морфологію плівок MEH-PPV/*nc*-ZnO. Найкраща фазова сумісність спостерігається для MEH-PPV і *nc*-ZnO при використанні модифікаторів (PI1) і (PI2). Використання модифікаторів призводить до зниження гасіння часу життя флуоресценції (τ_1) та збільшенню ефективності переносу заряду (η_q). Показано, що використання усіх модифікаторів призвело до збільшення J_{SC} та V_{OC}.

1. Introduction

A bulk heterojunction (BHJ) photovoltaic (PV) device on the base of hybrid photoactive films comprising the photosensitivity polymer (donor) and semiconductor nanocrystals (acceptor) are of great interest as an alternative for Si based energy sources [1]. BHJ photovoltaic cells usually include a large number of donor/acceptor interfaces for charge separation at the expense of discontinuous transport pathways by hopping. In these hybrid photovoltaic cells the recombination occurs almost exclusively at the heterojunction and the exciton dissociation efficiency is strongly dependent on the type of nanocrystals dispersion or phase segregation in polymer matrix, which are thereby crucial for the PV device performance. Thus, one of the key issues for fabrication of the efficient photovoltaic devices is morphology control of the BHJ active layer [2–5].

Usually these processes can be controlled by nanoparticles surface modification with suitable surfactants (interface modifiers, IMs) [6, 7]. Structure of the typical IMs consists of polar thiol-, amino-, mercapto- or phosphonic heads as anchoring groups, and conjugated molecular backbone [8]. Role of the IMs reveals in enhancement of the chemical compatibility between polymer and semiconductor nanoparticles, increasing the excitons separation efficiency at the polymer/nanoparticle interface and subsequent charge transfer rate into the nanoparticle bulk, reduction of interfacial recombination and improvement of a charge transport in polymer matrix as a result of the macromolecules ordering in the polymers [9].

As promising candidates for conjugated backbone groups, oligoarenes and organic dyes can be considered. However, only several research groups modified the surface of metal-oxide nanoparticles with different dyes: mercurochrome [10], N719 dye [11], as well as 2-amino-1-methylbenzimidazole [8], 2-naphthalenethiol (2-NT) [9], anthracene-9-carboxylic acid (ACA), tetracarboxy phthalocyanine copper (II) (CuPc-dye) and N3-dye [12], oligothiophenic phosphonic acids [13] and peryleneimide dyes (PIs) [14–17]. As a result, substantial improvement in short-circuit current density (J_{SC}), open-circuit voltage (V_{OC}) and fill factor (FF) of the modified device were obtained. Influence of the chemical structure of phosphonic acid containing interface modifiers of TiO_2 on photoinduced properties of the layered-junction

TiO_2/IMs/P3HT was investigated in [13]. Both photoluminescence (PL) and PL lifetime measurements suggested that the photoinduced transfer of electrons from P3HT to TiO_2 increased as the conjugation length of molecular backbone increased or as the nonconjugated chain-length in IMs decreased. Moreover, molecular structure of the IMs strongly affected the photovoltaic cell performance of the layered device ITO/TiO_2/IM/P3HT/Au through their energy levels and charge transfer ability. The J_{SC} increased and V_{OC} reduced as number of thiophene rings increased and length of the insulating chain in the IMs decreased.

Peryleneimide dyes represent one of the most widely studied classes of organic semiconductors for applications in solid-state dye-sensitized solar cells (DSSCs) [14, 17]. It is known that the majority of organic conducting materials are *p*-type semiconductors whereas PIs are *n*-type semiconductors [18]. Such materials possess high electron mobility [19], specific carrier injection-tuning properties [20], large molar absorption coefficients [21] in combining with excellent photo [22] and thermal stabilities [23]. Physical properties of PI dyes can be tuned by introduction of appropriate substituents in imide or bay positions, which is important in design of the new materials for PV applications [15, 16]. A perylene derivative was used to enhance the photoelectric efficiency of the hybrid poly(3-hexylthiophene)/ZnO bulk-heterojunction solar cells [17].

Although most of the cited above works are devoted to application of the PI dyes as sensitizers in DSSCs, effect of the PI dyes as the IMs on the active layer morphology and photovoltaic properties of solar cells was not studied practically. We know one work only devoted to the effect of perylen dye (perylenetetracarboxylic acid diimide) ligand shell formed on Au nanoparticles on morphology of the active layer and photovoltaic properties of solar cells [24].

In this work, we study the effects of the interface modifiers formed at ZnO nanocrystals surface on the MEH-PPV/ZnO-nanocrystals morphology, luminescence and photovoltaic properties of the photoactive layers in polymer-inorganic BHJ photovoltaic cells.

2. Experimental

Colloid solution of ZnO nanocrystals stabilized with methanol (native ligand shell) (*nc*-ZnO(Nat)) in cholorobenzene was ob-
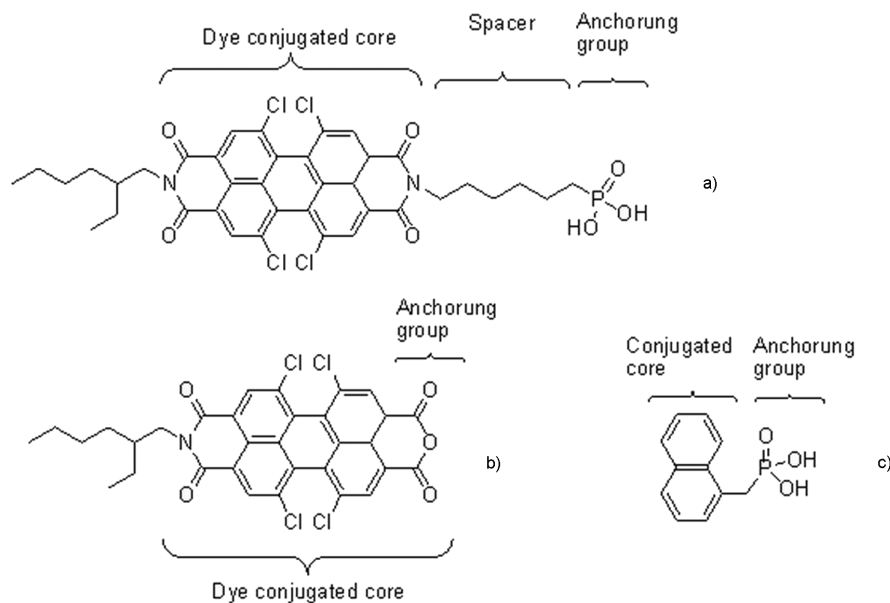
Fig. 1. Structures of IM: a — PI1, b — PI2 and c — NPA.

tained using method described previously in [25], the nanocrystal average size was ~ 3.5 nm, as was determined by TEM. Concentration of *nc*-ZnO(Nat) in the colloids was 60 mg·ml^{-1}. Photosensible conjugated polymer MEH-PPV, chlorobenzene and ITO glass substrates were purchased from Sigma-Aldrich, Inc. The polymer had the number average molecular weight, $M_n =$ 40,000–70,000 and polydispersity (M_w/M_n) of about 5.

Unsymmetrical substituted perylene imide dyes N-(2-ethylhexyl)-N′-(6-phos-phono-hexyl)-1,6,7,12-tetrachloro-perylene -3,4,9,10 -tetracarboxylic acid bisimide (PI1) and N-(2-ethylhexyl)-1,6,7,12-tetrachloroperylene-3,4,9,10-tetracarboxylic acid-3,4-anhydride-9,10-imide (PI2) were synthesized starting from 3,4,9,10-tetracar-boxylic acid-3,4,9,10-dianhydride similarly to described in [26]; details of the synthesis and isolation of target compounds will be published elsewhere. We used 1-naphthyl phosphonic acid (NPA) (Sigma-Aldrich) also to compare effect of small conjugative molecules without a long alkyl chains. ZnO nanocrystals with modified surface (*nc*-ZnO(IM)) were obtained via heating of *nc*-ZnO colloids with an excess of appropriate surfactants (IM) at 50°C for 20 h similarly as it was described in [27].

Blend films were prepared by adding colloid solution of modified *nc*-ZnO(IM), to MEH-PPV solutions in chlorobenzene at concentration of 6 mg/ml. The mass ratio of MEH-PPV/*nc*-ZnO was of 1:2. A typical

MEH-PPV/*nc*-ZnO(IM) film thickness was 70–80 nm.

Reduction E_{red} and oxidation E_{ox} potentials of the IMs were determined by cyclic voltammetry (CV) measurements (CH instruments (797 VA Computrace)) at a scan rate of 0.1 V/s at the room temperature. Morphology of the MEH-PPV/NC(IM) blend films with ZnO-IM nanocrystal was studied by transmission electron microscopy (TEM), using Selmi TEM-125 microscope. Photoluminescence spectra were recorded using SDL-2 (LOMO, Russia) double-monochromator spectrometer. Fluorescence lifetimes were detected by a sub-nanosecond kinetic spectrometer, consisting of MDR-12 monochromator (LOMO, Russia), TimeHarp 200 TCSPC device, PLS 340-10 picosecond LED driven by PDL 800-B device (PicoQuant GmbH, Germany) and Hamamatsu H5783P PMT (Hamamatsu, Japan). $J–V$ characteristics were measured on the photovoltaic cells with the architecture ITO/PEDOT-PSS/photoactive layer/Al with Amper-voltmeter W7-35 under 100 mW·cm^{-2} illuminations from a 100 W tungsten-halogen lamp. All measurements were performed at the ambient conditions.

3. Results and discussion

Structures of the studied interface modifier molecules (PI1, PI2 and NPA) are distinguished in the length of spacer, nature of anchoring group and expansion of conjugated π-electronic system (see Fig. 1). In order to reduce the tendency of perylenic

Table 1. Results of cyclic voltammetry

IM	E_{red}, eV	E_g, eV	E_{LUMO}, eV	E_{HOMO}, eV
PI1	−0.72	2.14	−3.67	−6.10
PI2	−0.51	2.23	−3.89	−6.23
NPA	−1.01	3.73	−3.38	−7.3

IMs to aggregates formation [28], and thereby to enhance the photoelectron transfer injection from the IMs to nc-ZnO and consequently to increase the J_{SC} values [29, 30], the structures of the chosen dyes contain four chlorine atoms in the bay position and branched terminal alkyl chain.

In order to determine the IMs reduction potential (E_{red}) the cyclic voltammetry measurements were performed. HOMO and LUMO values of the IMs were estimated using equations [31]: $E_{LUMO} = [(E_{red} - E_{1/2(\text{ferrocene})} + 4.8]$ and $E_{HOMO} = E_{LUMO} - E_g$, where $E_{1/2(ferrocene)}$ is the average of the oxidation potential of ferrocene as an external standard. Results of the cyclic voltammetry are presented in Table 1.

In BHJ devices the hybrid films morphology is one of the key parameters in achieving the device optimal performance. The TEM pattern for the blend films is different essentially for various IMs (see Fig. 2a–2d). When nc-ZnO coated with the native ligand shell (i.e. as synthesized) are used (nc-ZnO(Nat)), the phase segregation in MEH-PPV/nc-ZnO(Nat) films is observed, i.e. nc-ZnO form the aggregates comprising close-packed nanoparticles (Fig. 2a). The distance between these aggregates exceeds considerably the exciton diffusion length L_d ~ 10 nm in MEH-PPV polymer [32]. In the MEH-PPV/nc-ZnO(NPA) blend film the phase segregation also takes place (Fig. 2b). However, the adjacent ZnO nanocrystals in the aggregates are separated by thin polymer layer of ~ 6 nm thickness which is less than L_d. In contrast to the both above-mentioned blend films, in the case of MEH-PPV/nc-ZnO(PI2) blend films the phase segregation occurs on a nanometer scale (Fig. 2d), i.e. the small sized rod-like aggregates of nc-ZnO are formed which are distributed homogeneously in the polymer matrix. Finely, the random distribution of nc-ZnO(PI1) is observed for the MEH-PPV/nc-ZnO(PI1) blend films. It can be assumed that the bulkier molecules of PI1 and PI2, in comparison with NPA, provide an effective interaction with polymer host and thus prevent the nanocrystals ag-
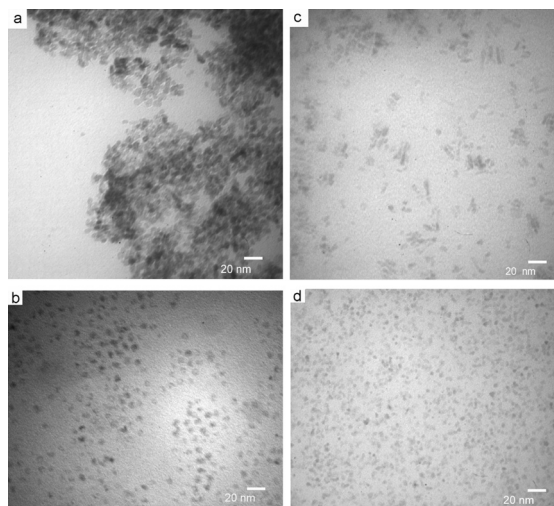

Fig. 2. TEM image of MEH-PPV/nc-ZnO(IM) blend films, containing ZnO nanocrystals with different interface modifiers: a — IM(Nat); b — IM(NPA); c — IM(PI2); d — IM(PI1).

gregation and macroscopic phase separation in course of the film preparation. Thus, the phase states of polymer/nc-ZnO(IM) blend films can be controlled with the balance between number and size of aliphatic and aromatic fragments in the IMs molecules.

To examine the effect of interface modification on charge carrier transfer, the time-resolved photoluminescence (TRPL) and photoluminescence quenching measurements in the bulk (BHJ) and bilayer (BLHJ) heterojunction device configurations were performed. Using the BLHJ configuration allowed to eliminate influence of the phase segregation and charge collection effects [33] and to study the effect of the IM chemical structure on exciton decay in MEH-PPV/nc-ZnO(IM) heterostructures only.

In order to elucidate the relaxation dynamics in our blend films the TRPL measurements were performed. The data obtained by the least-squares fit revealed that all PL transient traces for MEH-PPV/nc-ZnO(IM) films with different IMs decay as bi-exponential function $I(t) = I_{10} \cdot \exp(-t/\tau_1) + I_{20} \cdot \exp(-t/\tau_2)$, where τ_1 and τ_2 are fluorescence quenching lifetimes corresponding to two relaxation processes: a fast decay (τ_1) due to exciton dissociation at the MEH-PPV/nc-ZnO(IM) interfaces and a slow decay (τ_2) due to their direct recombination in the polymer bulk [34]. Presumably, the presence of pure MEH-PPV regions (free of nc-ZnO) with sizes bigger than L_d, is the origin of I_{02} quenching component in $I(t)$ and

Table 2. Time-resolved photoluminescence and photoluminescence quenching characterictics of bilayer (**BLHJ**) and bulk (**BHJ**) heterojunction MEH-PPV/ZnO-NC containing ZnO nanocrystals with different IMs

Active layer	Type of hetero junction	η_q BZ ZA, a.u.	η_{BHJ}/η_{BLHJ}, a.u.	τ_1, ps	I_{10}/I_{20}, a.u.
MEH-PPV/NC(Nat)	BLHJ	0.17	–	348	–
MEH-PPV/NC(Nat)	BHJ	0.21	1.23	350	2.21
MEH-PPV/NC(NPA)	BLHJ	0.45	–	334	–
MEH-PPV/NC(NPA)	BHJ	0.59	1.31	319	3.02
MEH-PPV/NC(PI1)	BLHJ	0.38	–	312	–
MEH-PPV/NC(PI1)	BHJ	0.94	2.57	301	10.64
MEH-PPV/NC(PI2)	BLHJ	0.47	–	218	–
MEH-PPV/NC(PI2)	BHJ	0.87	1.82	207	27.4

nonzero τ_2 at the TRPL measurements as well residual PL intensity at the PL quenching measurements. As it was found for the blend films containing surface-modified *nc*-ZnO, the parameter τ_1 depends from the type of IM molecules. Variation of τ_2 is apparently attributed to the changing of the molecular structure of a polymer matrix at the intercalation of the nanoparticles owing to polymer/*nc*-ZnO(IM) interaction [34]. In addition, the value of I_{10}/I_{20}, determining the relative contribution of fast and slow decay relaxation processes in the TRPL, depends on the IM type essentially. The reduced PL-decay lifetime for *nc*-ZnO(PI2) relatively *nc*-ZnO(Nat), *nc*-ZnO(PI1) and *nc*-ZnO(NPA) indicated the more rapid charge transfer from the polymer to *nc*-ZnO with IM(PI2) than with other modifiers.

The PL quenching efficiencies (η_q) are defined as $\eta_q = 1 - (A_{IM}/A_0)$, where A_{IM} and A_0 denote the area under the PL curves of MEH-PPV/*nc*-ZnO(IM$_i$)/substrate and pristine MEH-PPV/substrate, respectively [13]. The obtained PL quenching efficiency for BLHJ and BHJ as well lifetimes and ratio I_{10}/I_{20} for the studied samples are presented in Table 2. The greatest η_{BLHJ}(PI2) = 0.47 and η_{BLHJ}(NPA) = 0.45 are for PI2 and NPA molecules, while for Nat and PI1 modifiers η_{BLHJ} are less, 0.17 and 0.38, correspondingly. Therefore, we have concluded that the transfer carriers efficiency is higher for the IM(PI2) than for IM(Nat) and IM(PI1), if not to take into account the effect of NC distribution in MEH-PPV matrix.

As it follows from Table 2, the highest and almost equal values of quenching luminescence efficiency η_q for BHJ cells are observed for IM(PI1) 0.94, and IM(PI2) 0.87,

while PL-decay lifetime τ_1 = 207 ns is essentially smaller for IM(PI2) than for IM(PI1). This reveals that despite of the highest velocity of the charge transfer process from MEH-PPV macromolecules to ZnO nanocrystals with IM(PI2) in comparison with IM(PI1), the efficiency of an electron transfer in MEH-PPV/*nc*-ZnO(PI2) blend film, comprising the small size rod-like ZnO aggregates, is smaller than for MEH-PPV/NC(PI1) blend film, where *nc*-ZnO are distributed randomly.

It is worth to note that the decay lifetime τ_1 values for BHJ and BLHJ cells with the same IMs are similar in contrast to the PL quenching efficiencies (η_q) which depend on cell configurations. In the BLHJ cell configuration the quenching efficiency η_q is determined by the IM molecular structure only. On the contrary, in the BHJ cell configuration η_q values depend on the blend film morphology. The η_{BHJ}/η_{BLHJ} ratio allows to eliminate the contribution in η_{BHJ} of molecular and energy structure of the IM and evaluate contribution of the film morphology only. From Table 2 is seen that η_{BHJ}/η_{BLHJ} value (2.57) is the highest for IM(PI1) and corresponds to the homogeneous distribution of *nc*-ZnO. The values of I_{10}/I_{20} ratio are in a good compliance with η_{BHJ}/η_{BLHJ} for the same IMs. For IMs PI1 and PI2 the I_{10}/I_{20} ratio is much higher, than for native surfactant and NPA. This means that the electron transfer from MEH-PPV to ZnO-NC gives the primary contribution in the PL decay process comparing to contribution of the direct exciton recombination in the polymer bulk. Thus, in the both types of MEH-PPV blend films doped with *nc*-ZnO(PI1) and *nc*-ZnO(PI2) a signifi-

Table 3. Device performances of ITO/PEDOT:PSS/MEH-PPV:*nc*-ZnO(IMs)/Al hybrid photovoltaic devices with different interface modifiers

Active layer	J_{SC}Б		
MEH-PPV/NC(Nat)	8.1	192	20
MEH-PPV/NC(NPA)	23.7	461	23
MEH-PPV/NC(PI1)	13.7	244	20
MEH-PPV/NC(PI2)	26.4	605	24

cant part of the photogenerated excitons can reach the nanocrystals interface within their natural lifetime owing to nanoparticle dispersion state in the polymer host. Decrease of η_{BHJ}/η_{BLHJ} ratio means that phase separation arises in the blend system. The trend in direct correlation between the η_{BHJ}/η_{BLHJ} data and the film morphology are also retained for the MEH-PPV films containing *nc*-ZnO(Nat) and *nc*-ZnO(NPA). From Fig. 2a and 2b it follows that the *nc*-ZnO aggregates are formed in the both MEH-PPV/*nc*-ZnO(Nat) and MEH-PPV/*nc*-ZnO(NPA) films; the η_{BHJ}/η_{BLHJ} values decrease when molecules (PI1) or (PI2) are used as the IMs.

We have also evaluated the overall photovoltaic ITO/PEDOT:PSS/MEH-PPV:*nc*-ZnO(IM)/Al devices performance from the measured current-voltage ($J-V$) characteristics (Fig. 3) and results for the best set of devices are summarized in Table 3.

These results indicate that the photovoltaic performance is improved considerably by modifying the interfaces of MEH-PPV/*nc*-ZnO with NPA and PI2 ligands. Among these devices a solar cell that comprises *nc*-ZnO modified by PI2 demonstrates the best device performance with $J_{SC} = 26.4$ µA/cm^2, $V_{OC} = 605$ mV, and $FF = 24$ %. Unfortunately, due to relatively narrow spectral absorption range and low holes mobility in the MEH-PPV host as well nonoptimized *nc*-ZnO(IM) concentration and thick of the nanocomposite active layer, the power conversion efficiency was rather low value for all devices.

Comparison of the device performance results allows to suggest that the large improvement in J_{SC}, V_{OC} obtained using PI2 can be attributed to lower located LUMO levels than that for Nat or PI1. Lowering of energy barrier for electron injection between MEH-PPV and *nc*-ZnO, when IMs with lower located LUMO level are used, result in increase of the current density and to decrease of V_{OC} [14]. Instead, the V_{OC} values increase symbatically with J_{SC}.
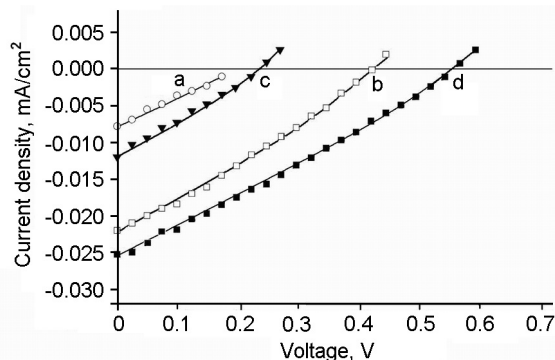

Fig. 3. $J-V$ curves of the ITO/PEDOT:PSS/MEH-PPV:*nc*-ZnO(IM)/Al cells, containing ZnO nanocrystals in the active layer with: a — IM(Nat); b — IM(NPA); c — IM(PI1); d — IM(PI2).

Therefore it can be supposed that PI2 molecules serve as the recombination barriers [13] resulting in the raise of electron and hole concentrations at MEH-PPV/*nc*-ZnO interfaces. This leads to increase of the difference between the quasi-Fermi levels of electrons and holes, and hence to increase in V_{OC}. At the same time IM can influence on back recombination kinetics: the IM molecules are more bulky and less planar, the more effective barrier to the back recombination take place [35, 36].

4. Conclusions

In this work MEH-PPV/*nc*-ZnO(IMs) nanocomposite films have been fabricated as an active layer for solar cells. The obtained results show that the *nc*-ZnO interfacial modification is crucial for the blend film morphology and device performance. Specifically, the IM molecular structure strongly affected the fluorescence lifetime quenching (τ_1) and the quenching efficiencies (η_q) of the BLHJ photovoltaic cells by their energy levels and charge transfer ability. It is found that the IMs can control the phase separation degree of donor and acceptor phases. It is shown that the bulkier molecules of PI1 and PI2, in comparison with the native surfactant and NPA, pro-

vide effective interaction with the polymer host and thus prevent the nanocrystals aggregation and macroscopic phase separation in the course of the film preparation. All studied herein IMs increase considerably the *PCE*, suggesting the IMs improve essentially the MEH-PPV/*nc*-ZnO interface, promoting dissociation of excitons in the polymer matrix.

References

1. Y.Y.Lin, T.H.Chu, C.W.Chen, W.F.Su, *J. Appl. Phys. Lett.*, **92**, 0533121 (2008).
2. M.H.Yum, G.H.Kim, C.Yang, J.Y.Kim, *J. Mater. Chem.*, **20**, 7710 (2010).
3. M.A.Ruderer, S.Guo, R.Meier et al., *Adv. Funct. Mater.*, **21**, 3382 (2011).
4. L.J.A.Koster, O.Stenzel, S.D.Oosterhout et al., *Adv. Ener. Mater.*, **3**, 615 (2013).
5. J.Liu, W.Wang, H.Yu et al., *Sol. Energy Mater. Sol. Cells.*, **92**, 1403 (2008).
6. P.Ravirajan, A.M.Peir, M.K.Nazeeruddin et al., *J. Phys. Chem.*, **B 110**, 7635 (2006).
7. C.Goh, S.R.Scully, M.D.McGehee, *J. Appl. Phys.*, **101**, 1145031 (2007).
8. N.Balis, V.Dracopoulos, E.Stathatos et al., *J. Phys. Chem. C*, **115**, 10911 (2011).
9. J.-Y.Chen, F.-C.Hsu, Y.-M.Sungc, Y.-F.Chenc, *J. Mater. Chem.*, **22**, 15726 (2012).
10. Y.-Y.Lin, Y.-Y.Lee, L.Chang et al., *Appl. Phys. Lett.*, **94**, 063308 (2009).
11. R.Thitima, C.Patcharee, S.Takashi, Y.Susumu, *Solid-State Electron.*, **53**, 176 (2009).
12. Y.-Y.Lin, T.-H.Chu, S.-S.Li et al., *J. Am. Chem. Soc.*, **131**, 3644 (2009).
13. Ch.-W.Hsu, L.Wang, W.-F.Su, *J. Coll. Inter. Sci.*, **329**, 182 (2009).
14. S.Erten-Ela, G.Turkmen, *Renewable Energy*, **36**, 1821 (2011).
15. E.Kozma, M.Catellani, *Dyes and Pigments*, **98**, 160 (2013).
16. H.Dincalp, Z.As, C.Zafer, S.Icli, *Dyes and Pigments*, **91**, 182 (2011).
17. M.Wang, X.Wang, *Sol. Energy Mater. Sol. Cells*, **92**, 766 (2008).
18. S.Vajiravelu, R.Lygaitis, J.V.Grazulevicius et al., *J. Mater. Chem.*, **19**, 4268 (2009).
19. B.A.Jones, A.Facchetti, M.R.Wasielewski, T.J.Marks, *J. Amer. Chem. Soc.*, **129**, 15259 (2007).
20. J.Pan, W.Zhu, S.Li et al., *Eur. J. Org. Chem.*, **4**, 986 (2006).
21. C-C.Chao, M-K.Leung, Y.O.Su et al., *J. Org. Chem.*, **70**, 4323 (2005).
22. H.Dincalp, S.Icli, *Solar Energy*, **80**, 332 (2006).
23. S.Becker, A.Bohm, K.Mullen, *Chemistry*, **6**, 3984 (2000).
24. J.Li, X.-L.Yu, J.Fu et al., *J. Chem. Sci.*, **122**, 839 (2010).
25. W.J.E.Beek, M.M.Wienk, R.A.J.Janssen, *Adv. Mater.*, **16**, 1009 (2004).
26. H.Troster, *Dyes and Pigments*, **4**, 171 (1983).
27. M.F.Prodanov, N.V.Pogorelova, A.P.Kryshtal et al., *Langmuir*, **29**, 9301 (2013).
28. Ch.Huang, S.Barlow, S.R.Marder, *J. Org. Chem.*, **76**, 2386 (2011).
29. J.Liu, W.Wang, H.Yu et al., *Sol. Energ. Mater. Sol. Cells.*, **92**, 1403 (2008).
30. H.Langhals, O.Krotz, K.Polborn, P.Mayer, *Angew., Chem. Int. Ed.*, **44**, 2427 (2005).
31. J.Pommerehene, H.Vestweber, W.Guss et al., *Adv. Mater.*, **7**, 551 (1995).
32. A.J.Lewis, A.Ruseckas, O.P.M.Gaudin et al., *Org. Electron.*, **7**, 452 (2006).
33. K.M.Coakley, Y.Liu, M.D.McGehee et al., *Adv. Funct. Mater.*, **13**, 301 (2003).
34. J.-Yu.Chen, F.-Ch.Hsu, Yu-M.Sung, Y.-F.Chen, *J. Mater. Chem.*, **22**, 15726 (2012)
35. C.Zafer, M.Kus, G.Turkmen et al., *Sol. Energ. Mater. Sol. Cell.*, **91**, 427 (2007).
36. A.Burke, S.Ito, H.Snaith, *Nano Lett.*, **8**, 977 (2008).